Atmos. Meas. Tech., 9, 5203–5212, 2016
www.atmos-meas-tech.net/9/5203/2016/
doi:10.5194/amt-9-5203-2016

Atmospheric Measurement Techniques
Open Access
EGU

Comparison of OMI NO_2 observations and their seasonal and weekly cycles with ground-based measurements in Helsinki

Iolanda Ialongo[1], Jay Herman[2], Nick Krotkov[2], Lok Lamsal[2,3], K. Folkert Boersma[4,5], Jari Hovila[1], and Johanna Tamminen[1]

[1]Earth Observation Unit, Finnish Meteorological Institute, Helsinki, Finland
[2]Atmospheric Chemistry and Dynamics Laboratory, NASA Goddard Space Flight Center, Greenbelt, Maryland, USA
[3]GESTAR, Universities Space Research Association, Columbia, Maryland, USA
[4]Royal Netherlands Meteorological Institute, Climate Observations Department, De Bilt, the Netherlands
[5]Wageningen University, Meteorology and Air Quality Group, Wageningen, the Netherlands

Correspondence to: Iolanda Ialongo (iolanda.ialongo@fmi.fi)

Received: 20 June 2016 – Published in Atmos. Meas. Tech. Discuss.: 22 June 2016
Revised: 15 September 2016 – Accepted: 6 October 2016 – Published: 24 October 2016

Abstract. We present the comparison of satellite-based OMI (Ozone Monitoring Instrument) NO_2 products with ground-based observations in Helsinki. OMI NO_2 total columns, available from NASA's standard product (SP) and KNMI DOMINO product, are compared with the measurements performed by the Pandora spectrometer in Helsinki in 2012. The relative difference between Pandora no. 21 and OMI SP total columns is 4 and −6 % for clear-sky and all-sky conditions, respectively. DOMINO NO_2 retrievals showed slightly lower total columns with median differences about −5 and −14 % for clear-sky and all-sky conditions, respectively. Large differences often correspond to cloudy fall–winter days with solar zenith angles above 65°. Nevertheless, the differences remain within the retrieval uncertainties. The average difference values are likely the result of different factors partly canceling each other: the overestimation of the stratospheric columns causes a positive bias partly compensated by the limited spatial representativeness of the relatively coarse OMI pixel for sharp NO_2 gradients. The comparison between Pandora and the new version (V3) of OMI NO_2 retrievals shows a larger negative difference (about −30 %) than the current version (V2.1) because the revised spectral fitting procedure reduces the overestimation of the stratospheric column.

The weekly and seasonal cycles from OMI, Pandora and NO_2 surface concentrations are also compared. Both satellite- and ground-based data show a similar weekly cycle, with lower NO_2 levels during the weekend compared to the weekdays as a result of reduced emissions from traffic and industrial activities. The seasonal cycle also shows a similar behavior, even though the results are affected by the fact that most of the data are available during spring–summer because of cloud cover in other seasons.

This is one of few works in which OMI NO_2 retrievals are evaluated in a urban site at high latitudes (60° N). Despite the city of Helsinki having relatively small pollution sources, OMI retrievals have proved to be able to describe air quality features and variability similar to surface observations. This adds confidence in using satellite observations for air quality monitoring also at high latitudes.

1 Introduction

Nitrogen oxides ($NO_x = NO + NO_2$) play an important role in tropospheric chemistry, participating in ozone and aerosol production processes. NO_x is mainly generated in polluted regions by anthropogenic combustion and it is toxic when present at high concentrations at the surface.

The NO_2 content in atmosphere can be monitored using satellite observations. Satellite-based NO_2 total and tropospheric columns have been available since 2004 from the Dutch–Finnish Ozone Monitoring Instrument (OMI), onboard NASA's EOS (Earth Observing System) Aura satellite (Levelt et al., 2006). OMI provides almost daily global

coverage with a nominal spatial resolution of $13 \times 24\,km^2$ at nadir.

Satellite instruments provide global NO_2 observations used in several air quality applications including recent studies on emission and lifetime estimation (Beirle et al., 2011; de Foy et al., 2015; Lu et al., 2015; Liu et al., 2016; McLinden et al., 2016), emission changes (Castellanos and Boersma, 2012; McLinden et al., 2012; Hilboll et al., 2013; Duncan et al., 2013; Krotkov et al., 2016), ship emission monitoring (de Ruyter de Wildt et al., 2012; Ialongo et al., 2014) and satellite-constrained NO_x emission inventories (Lamsal et al., 2011; Ghude et al., 2013; Streets et al., 2013; Vinken et al., 2014). Satellite data have also been used for urban pollution monitoring, e.g., looking at the NO_2 weekly cycle (Beirle et al., 2003; Boersma et al., 2009). The results of these studies are strongly affected by the accuracy of the satellite retrievals; thus accurate validation against independent ground-based measurements is continuously needed.

Recently, the Pandora instrument has been developed to help in evaluating satellite NO_2 retrievals with ground-based measurements (Herman et al., 2009). The Pandora spectrometer system measures direct sunlight in the UV–VIS (ultraviolet–visible) spectral range (280–525 nm). It provides NO_2, O_3 and SO_2 total columns through the direct-sun DOAS (differential optical absorption spectroscopy) technique. This technique provides very accurate NO_2 observations, compared to zenith sky measurements, because it does not require complex prior assumptions for converting the slant columns into vertical columns. Because Pandora is a low cost instrument, it is largely applied for satellite-data validation, and the observation network is quickly growing (see http://acdb-ext.gsfc.nasa.gov/Projects/Pandora/index.html).

Lamsal et al. (2014) extensively evaluated the current version of OMI NO_2 retrievals using several different ground-based observations, including Pandora measurements. They found that OMI and Pandora NO_2 total columns are fairly correlated ($r = 0.25$) and in agreement to within 30 %. Before that, Pandora measurements had been used for evaluating OMI NO_2 total columns also by Herman et al. (2009) and Tzortziou et al. (2013). In addition, Knepp et al. (2013) estimated surface NO_2 mixing ratios from Pandora measurements and found high correlation (typically $r > 0.75$) with surface records from a photolytic-converter-based instrument.

Most of the validation studies are performed at midlatitude or low-latitude sites, and a detailed evaluation of OMI NO_2 products at higher latitudes is still missing. High latitudes, and in particular the Arctic, are becoming more and more important because of the increasing anthropogenic activities foreseen in these regions (e.g., new oil extraction and mining sites, new shipping routes as well as urban emissions). Satellite-based observations offer a unique opportunity for monitoring atmospheric composition in such remote areas with very sensitive environments. Thus, the quality of atmospheric observations needs to be continuously evaluated in order to provide reliable retrievals.

This work aims to evaluate the quality of OMI NO_2 products through comparison with ground-based observations in Helsinki (Finland), which is the northernmost city (latitude of 60.2° N) with more than half a million inhabitants. The database used in the analysis is described in Sect. 2. The results of the comparison of OMI NO_2 total columns with ground-based Pandora observations are shown in Sect. 3.1. OMI NO_2 seasonal and weekly cycles are also compared to those derived from surface concentrations from air quality stations in Sect. 3.2. Finally, the summary and conclusions are presented in Sect. 4.

2 NO_2 observations

2.1 OMI NO_2 products

In this work, OMI NO_2 total and tropospheric column densities are taken into account. OMI is a Dutch–Finnish instrument, which has been operating on board NASA's Aura satellite since October 2004. OMI measures solar backscattered light in the UV–VIS spectral region using a two-dimensional CCD (charge-coupled device) detector. The cross-track swath is divided into 60 pixels. The nominal resolution at nadir (row 30) is $13 \times 24\,km^2$, with increasing pixel size towards the edges of the swath (up to $28 \times 150\,km^2$). The Aura satellite flies in a sun-synchronous polar orbit with nominal Equator crossing time 13:45 LT with almost daily global coverage. At high latitudes more than one daily overpass can be obtained because of the overlapping orbits. Since 2007 the so-called "row anomaly" affected some of the cross-track positions of the swath, reducing the spatial coverage of the instrument. In this work, the affected rows are removed according to the operational flagging for the row anomaly.

OMI NO_2 retrievals are obtained from the spectral measurements in the visible spectral range between 405 and 465 nm. There are two NO_2 products available from OMI: NASA's standard product (SP) version 2.1 (Bucsela et al., 2013) and KNMI's (Royal Netherlands Meteorological Institute) DOMINO (Derivation of OMI tropospheric NO_2) product version 2 (Boersma et al., 2011). Both retrievals are based on the DOAS technique but they differ in the way of converting the slant columns into vertical columns. Moreover, the separation between stratospheric and tropospheric columns is different. In the SP algorithm the stratosphere–troposphere separation is based on the OMI observations over areas with relatively little tropospheric NO_2, while the DOMINO algorithm assimilates OMI observations into a chemistry-transport model. Comprehensive validation of version 2.1 of OMI SP retrievals with independent measurements was presented by Lamsal et al. (2014) (and references therein). They showed that OMI retrievals are lower in urban regions and higher in remote areas, but generally in agree-

ment with ground-based and airborne measurements within ±20 %. The next-generation version 3 (V3) of the NO_2 standard product, based on the sequential DOAS fitting algorithm, is also used in the comparison to evaluate the overestimation of the stratospheric columns reported by Marchenko et al. (2015). The new V3 algorithm also includes monthly NO_2 vertical profiles from a higher-resolution (1° latitude by 1.25° longitude) chemistry-transport model simulation with time-dependent NO_2 emissions.

The Helsinki overpass SP data (available at http://avdc.gsfc.nasa.gov/) are taken into account in this study. The NO_2 retrievals from the DOMINO product corresponding to the same pixels as in the SP overpass file are obtained from the TEMIS website (http://temis.nl). The retrieval uncertainty for OMI NO_2 vertical column is on the order of 10^{15} molecules cm^{-2} for the Helsinki overpass dataset. Cloud fraction (CF) data from OMI are used to identify the almost cloud-free scenes. Both OMI NO_2 retrieval algorithms include the OMCLDO2 cloud product as input information, which is based on the O2–O2 absorption method (Acarreta et al., 2004). The pixels with surface reflectivity above 0.2 and with distance to the ground-based station larger than 50 km are removed from the analysis. Small-sized pixels (cross-track position 6–55) are also considered separately in the comparison.

The mean NO_2 tropospheric columns in Helsinki during May–September 2005–2014 are shown in Fig. 1. The mean NO_2 tropospheric column value goes up to about 3×10^{15} molecules cm^{-2}. This is about 5 times smaller than what can be observed for example in polluted areas in central Europe, and it is 6 times larger than the OMI detection limit ($\pm 5 \times 10^{14}$ molecules cm^{-2}). In addition to Helsinki, the main polluting sources in this area are the cities of Tallin and Turku, as well as emissions from ships in the Gulf of Finland (Ialongo et al., 2014).

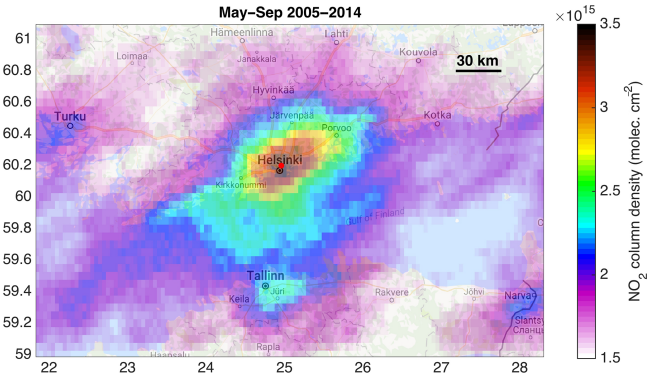

Figure 1. OMI NO_2 tropospheric column in Helsinki. The map shows the average over the time period 2005–2014 from May to September with 0.05° × 0.05° spatial resolution. The location of the ground-based station is shown as a red dot.

2.2 Ground-based observations

OMI NO_2 total columns are compared against ground-based observations performed during 2012 at the Helsinki-Kumpula station (60.20° N, 24.96° E), Finland, by the Pandora instrument no. 21. The measuring site is approximately located under the red dot in Fig. 1, corresponding to Helsinki. The Pandora system includes a spectrometer connected by a fiber optic cable to a sensor head with 1.6° FOV (field of view). A sun-tracking device allows the optical head to point at the center of the sun with 0.013° resolution. Pandora performs direct-sun measurements in the UV–VIS spectral range (280–525 nm), and provides NO_2, O_3 and SO_2 vertical column densities.

The algorithm first derives the relative NO_2 slant columns densities (SCDs) using the DOAS spectral fitting technique (e.g., Cede et al., 2006) in 370–500 nm (see Fig. 5 in Herman et al., 2009), and converts them to absolute SCDs using the statistically estimated reference spectrum obtained from on-site PANDORA measurements by the Langley extrapolation technique. Pandora SCD retrieval employs a temperature correction to the cross sections used in the spectral fitting procedure as described in Eq. (1) by Herman et al. (2009), based on modeled monthly average NO_2 and temperature profiles and high-resolution temperature-dependent cross sections by Vandaele et al. (1988), as also for OMI NO_2 retrievals.

The NO_2 columns are available about every 1.5 min. The full description of the Pandora instrument and the algorithm for the inversion methodology are reported by Herman et al. (2009). The nominal clear-sky precision in the Pandora NO_2 total column retrieval is on the order of 3×10^{14} molecules cm^{-2}, with an accuracy of about $\pm 1.3 \times 10^{15}$ molecules cm^{-2}. Ground-based cloud cover information from the ceilometer located at the Kumpula site (available at hav.fmi.fi) is used together with OMI CF cloud information, in order to identify the cloud-free scenes.

The NO_2 surface concentrations available at the Helsinki-Kumpula air quality station were used for the analysis of the seasonal and weekly cycle. The surface concentration data are obtained from the SMEAR database (Junninen et al., 2009), available online at avaa.tdata.fi/web/smart/smear. Kumpula station is classified as semi-urban because it is influenced by car pollution only downwind from the main high traffic street. The surface NO_2 concentrations are measured using an online trace-level gas analyzer based on the ultraviolet fluorescence method (i.e., European reference 5 method). Hourly average concentrations are used in this study. Only the measurements closest to the satellite overpass time (within 30 min) are taken into account. Note that the Pandora spectrometer is located on the roof of the FMI building, about 25 m above the air quality station (altitude about 4 m a.g.l.).

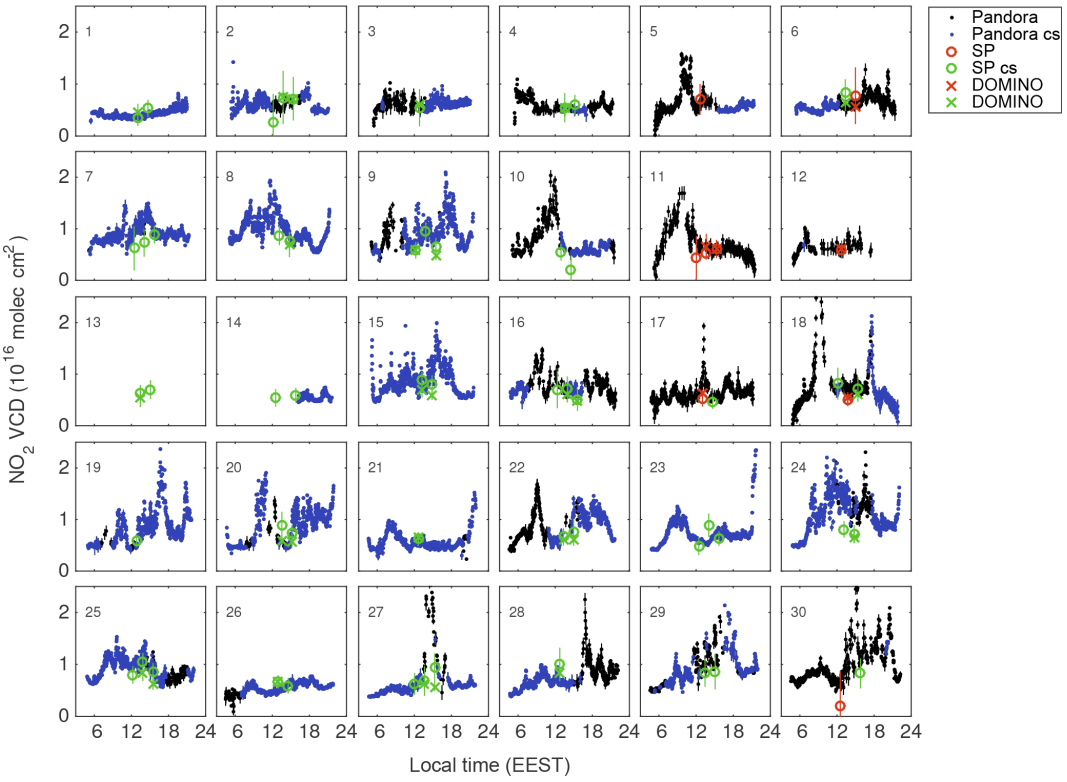

Figure 2. OMI and Pandora NO_2 total columns during May 2012. Both OMI SP and DOMINO data are shown. The day of the month is reported on the upper left corner of each subplot. OMI data are screened for clear-sky (cs) conditions using OMI CF < 0.5 (green circles and crosses for OMI SP and DOMINO, respectively), while Pandora clear-sky data (blue dots) are derived using cloud cover information from ceilometer (below 5/8). Pandora retrievals with uncertainties smaller than 1.3×10^{15} molecules cm^{-2} are shown.

3 Results

3.1 Comparison of OMI NO_2 total columns with Pandora observations

Figure 2 shows an example of the NO_2 total columns from Pandora and OMI overpasses during May 2012. Both OMI SP and DOMINO retrievals are included, with the former usually showing larger values than the latter. Pandora retrievals with uncertainty larger than 1.3×10^{15} molecules cm^{-2} are removed from the analysis. OMI data are cloud-screened according to OMI CF (below 0.5), while Pandora measurements are cloud-screened according to the ground-based cloud cover information from the ceilometer (below 5/8). These threshold values include clear-sky and partially cloudy scenes. These two cloud-screening criteria give similar results (see green symbols and blue dots in Fig. 2 for OMI and Pandora, respectively). When considering all the collocated data available in 2012, the cloud-screening criteria agree in more than 80 % of the cases. The uncertainty values in Pandora total columns are on average 3×10^{14} molecules cm^{-2} (or about 2 %), while the total column median of the uncertainties is about 1 order of magnitude larger for OMI retrievals (15–30 %).

Figure 2 also illustrates the measured diurnal variations in NO_2 total columns. The daily cycle is highly variable from day to day, depending on several factors, such as the diurnal cycle of anthropogenic NO_x emissions, NO_x photochemistry, relative contribution from stratospheric columns, as well as changing meteorological conditions. Under clear-sky conditions, Pandora NO_2 total columns show peaks in the morning or in the afternoon (as would be expected from increased car traffic during the rush hours and a small contribution from stratospheric columns). Sometimes, very low NO_2 total columns are observed throughout the day, as for example on 1 May 2012 (first panel in Fig. 2), probably because of the wind patterns. OMI overpasses occur between 12:00 and 15:30 local time (outside the rush hours), when relatively low tropospheric NO_2 levels are expected.

Figure 3 shows the difference between OMI SP and Pandora NO_2 total columns during 2012 as a function of CF, solar zenith angle (SZA), pixel area, distance between the city center and the center of the pixel, and Pandora NO_2 total column values. The median relative difference is (4 ± 19) and (-6 ± 25) % for clear-sky and all-sky conditions, respectively. These percentage values correspond to absolute differences $(3 \pm 11) \times 10^{14}$ and $(-4 \pm 18) \times 10^{14}$ molecules cm^{-2}, respectively. For the calculation of the clear-sky median both

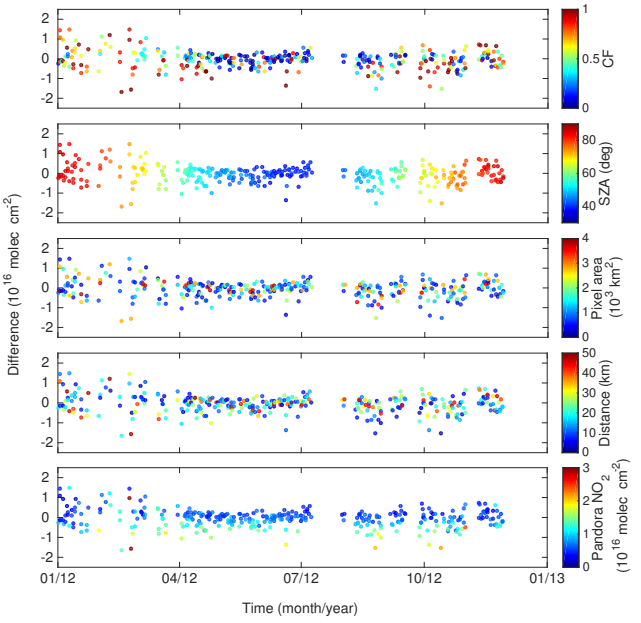

Figure 3. Difference between OMI SP and Pandora NO_2 total column in Helsinki during 2012. The color scales in the different panels correspond to OMI CF, SZA, pixel area, distance between the actual location of Pandora instrument and the center of OMI pixel, and Pandora NO_2 total column.

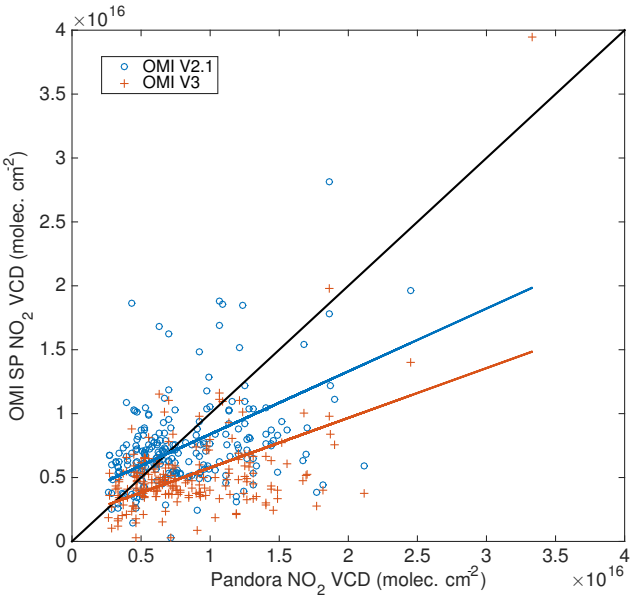

Figure 4. Scatter plot between OMI SP and Pandora NO_2 total column in Helsinki during 2012. Both version 2.1 and 3 of the OMI SP retrievals are shown (blue circles and red crosses, respectively), together with the corresponding linear fit (blue and red lines, respectively). The 1 : 1 line is indicated in black. Only pixels with cross-track position 6–55 are included.

criteria based on OMI CF and ground-based cloud cover are used to screen for the cloudy scenes. A similar comparison for the DOMINO product (Fig. S1 in the Supplement) shows that the median relative difference is (-5 ± 13) and (-14 ± 18) % for clear-sky and all-sky conditions, respectively (or in terms of absolute values $(-3 \pm 9) \times 10^{14}$ and $(-9 \pm 16) \times 10^{14}$ molecules cm^{-2}, respectively). The semi-interquartile is used to calculate the variability of the difference.

Winter–fall overpasses are often affected by clouds and also correspond to large SZA, increasing the uncertainty in the retrieval of the NO_2 total column. Data corresponding to spring–summer clear-sky days (SZA $< 65°$) show slightly smaller average difference (e.g., about 3 % for SP) compared to the value obtained from the whole dataset. One would also expect better agreement for small pixels and short distance between Helsinki city center and the center of the satellite pixel. This is not directly visible from Fig. 3 (third and fourth panels). However, there are a few cases with very large difference (outliers in Fig. 3) between OMI and Pandora, which correspond to high values of distance and pixel area. For example, the average relative difference between OMI SP and Pandora derived using relatively small pixels (cross-track position 6–55) is (-5 ± 25) %, about 1 % closer to zero than for the whole dataset (-6 ± 25) %.

These average values are the result of different effects, potentially canceling each other. For example, Belmonte Rivas et al. (2014), Marchenko et al. (2015) and van Geffen et al. (2015) reported that OMI slant column densities are high biased by about 10–40 %, producing an overestimation in the stratospheric vertical columns of the same order of magnitude (Adams et al., 2016). This causes the OMI retrievals to overestimate the total columns when compared to Pandora measurements. Marchenko et al. (2015) and van Geffen et al. (2015) proposed revisions of the spectral fitting in the OMI NO_2 retrieval algorithm, which reduce the slant column densities by 10–35 %, bringing them closer to independent measurements. The next-generation OMI NO_2 product (Version 3) accounts for this improved spectral fitting. Thus, in order to evaluate this positive bias, we compare Pandora total columns to a subset of data including both SP V2.1 and V3. The results are presented in the scatter plot in Fig. 4 for cross-track positions 6–55. The median relative difference for V3 is (-32 ± 18) % and it is much larger than for V2.1 (-5 %). The linear fit slopes are 0.49 and 0.39 for V2.1 and V3, respectively, and the correlation is moderate ($r = 0.51$ for both datasets). Such values are comparable to the values obtained for example by McLinden et al. (2014) and Kharol et al. (2015) using in situ surface observations. Slope values close to unity are not expected because of the different spatial resolution of satellite- and ground-based observations.

The difference between the OMI pixel and the relatively smaller Pandora FOV is indeed expected to cause an underestimation of the total column by OMI. This effect is analyzed in Fig. S2 in the Supplement, where the 2010 EDGARv4.3.1

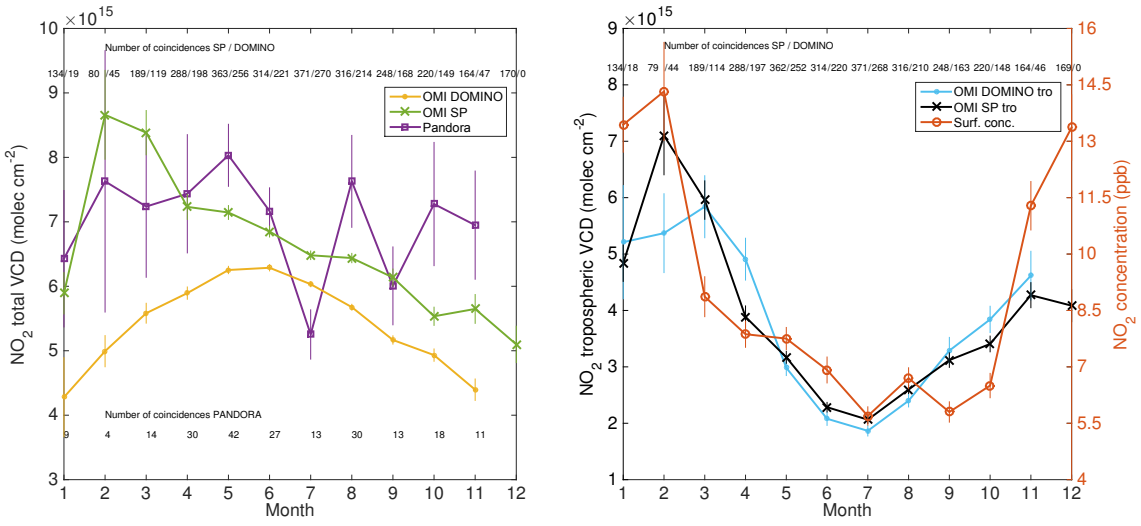

Figure 5. Left: NO_2 seasonal cycle from total columns from OMI SP and DOMINO (yellow) products during the period 2006–2014. The monthly means from collocated Pandora NO_2 total columns measured in Helsinki during 2012 are also shown (purple). Right: NO_2 seasonal cycle from tropospheric (tro) columns from OMI SP (black) and DOMINO (light blue) products. The seasonal cycle of the NO_2 surface concentrations measured in Kumpula air quality station is also shown in red. Note that VCDs (vertical column densities) and surface concentrations are reported on the left (molecules cm^{-2}) and right (ppb) y axis, respectively. The number of coincidences between OMI and the closest surface concentration measurement within 30 min is shown for each month on the top of both panels for both SP and DOMINO. The number of coincidences for the subset of Pandora observations is reported at the bottom of the left panel. The ground-based observations are sampled according to SP NO_2 products. The error bars are estimated from the standard deviation of the mean. Only collocated observations with OMI CF < 0.5 are taken into account.

NO_x emission map (available at http://edgar.jrc.ec.europa.eu) over Helsinki is presented. The outlines of three OMI pixels with different size (cross-track position 17, 53 and 60 with areas of 430, 870 and 3560 km^2, respectively) are overlapped to the emission map, in order to illustrate the effect of the relatively coarse spatial resolution. One must note that, because of the row anomaly, the smallest pixels at the center of the swath (close to cross-track position 30) are not available for the comparison. The emission estimate at the location of Pandora (red dot in Fig. S2) is about 5 ktons yr^{-1}. When averaging over OMI pixel area, the emission values decrease, while the size of the pixel increases. The emissions are about 20, 40 and 80 % smaller than the value at the Pandora location for pixel 17, 53 and 60, respectively. This difference in emissions is at least partially transferred to the vertical column (by a factor of about 0.8 according to Lamsal et al., 2011). Similarly, Irie et al. (2012) and Lin et al. (2014) found large discrepancies between space- and ground-based measurements especially over areas with high NO_2 spatial inhomogeneity, due to their different spatial representativeness. The comparison can also be affected by the position of the center of the OMI pixel compared to the ground-based station because different pixels sample different areas around the ground-based station. The OMI pixels included in the overpasses are distributed along the coastal line in the vicinity of Helsinki, and might include the contribution of marine atmosphere (e.g., ship emissions) or other pollution sources over land.

In addition, occasionally, Pandora NO_2 values build up to relatively high pollution levels (over 1.5×10^{16} molecules cm^{-2}). This likely occurs when the ground-based station is downwind from a main high traffic street. The difference between OMI and Pandora total columns shows relatively large negative values (OMI smaller than Pandora) for relatively large Pandora total columns (Fig. 3 – bottom panel), hinting that OMI is less able to reproduce such episodes of localized and elevated pollution because of the coarse pixel size. Overall, Pandora NO_2 total columns are expected to be larger than OMI retrievals because of the effect of the coarse OMI spatial resolution. This might partly cancel the positive bias caused by the overestimation of the stratospheric columns.

Furthermore, Vasilkov et al. (2016) analyzed the effect of the varying observation geometry on the NO_2 vertical column retrieval. They found that replacing the current OMI-based Lambertian-equivalent reflectivity (LER) climatology (Kleipool et al., 2008) used in OMI NO_2 algorithms with a high-resolution geometry-dependent LER based on MODIS (Moderate Resolution Imaging Spectroradiometer) observations causes an overall increase in the vertical column values over a test study orbit in the Americas. This effect could further change the bias we observe between OMI and Pandora retrievals.

It must be noted that there is a larger number of valid retrievals available from the SP product than from DOMINO

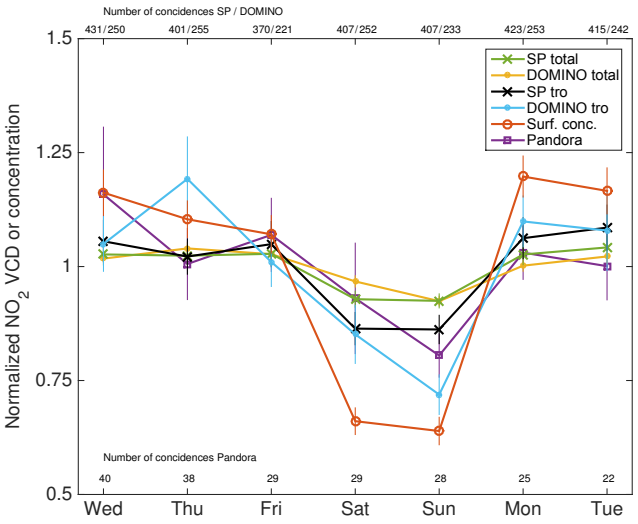

Figure 6. NO_2 weekly cycle from total and tropospheric columns from OMI SP (green and black, respectively) and DOMINO (yellow and light blue, respectively) products during 2006–2014. The weekly cycle of the NO_2 surface concentrations measured in Kumpula air quality station is also shown (red). The weekly cycle from collocated Pandora NO_2 total columns measured in Helsinki during 2012 is also shown (purple). The values for each day of the week are normalized with the weekly mean value in order to enhance the relative differences. The number of coincidences of OMI and the closest surface concentration measurement within 30 min are shown at the top of the figure for both SP and DOMINO. The number of coincidences for the subset of Pandora observations is reported at the bottom. The ground-based observations are sampled according to SP NO_2 products. The error bars are estimated from the standard deviation of the mean. Only observations with OMI CF < 0.5 are taken into account.

(especially during winter). This is caused by the fact that DOMINO retrievals are not available for SZAs larger than 80°. The different sampling only partly explains the observed difference between the median relative difference obtained from the two different OMI products. The remaining differences in the total columns from SP and DOMINO can be attributed to differences in air mass factor values (about 13 % smaller for OMI SP) used to convert the slant columns into vertical columns. Because the slant columns from SP and DOMINO are very similar to each others, the total column values from DOMINO algorithm are also found to be about 13 % smaller.

3.2 Analysis of the seasonal and weekly cycle

Figure 5 (left panel) shows the monthly means of the NO_2 total columns from OMI SP and DOMINO overpasses in Helsinki under almost clear-sky conditions (CF < 0.5). The monthly means from Pandora total columns available in 2012 are shown for comparison. Figure 5 (right panel) includes the NO_2 tropospheric columns and the surface concentrations from Helsinki-Kumpula air quality station (located a few meters from the Pandora spectrometer). Only coincident OMI overpasses and surface concentration data are included in the calculation of the monthly means. Because Pandora data are available for 1 year, the number of coincidences for the Pandora observations is smaller than for OMI and concentration data (see inset numbers in top and bottom axes in Fig. 5). In addition, the number of coincidences for SP is different than for DOMINO because of different assumptions for snow-covered surfaces and high solar zenith angles, which are recurring conditions at relatively high latitudes as in Helsinki (about 60° N). The error bars are determined as the standard deviation of the mean, and thus are larger for a decreasing number of coincidences.

The monthly means of tropospheric NO_2 and surface concentrations (Fig. 5 – right panel) show generally larger values in winter than in summer, as expected because of larger NO_x emissions, a shallower planetary boundary layer and a longer lifetime in winter. However, the total column monthly means derived from OMI and Pandora total columns (Fig. 5 – left panel) do not clearly show such a seasonal cycle. OMI DOMINO NO_2 total columns show different month-to-month variability compared to SP, with SP monthly means generally closer to Pandora values and larger than DOMINO. Additionally, Pandora monthly means (purple lines in the left panel in Fig. 5) are characterized by larger error bars and variability than the other datasets, as a result of the smaller number of data included in the calculation. The results are strongly affected by the fact that the number of available data is up to 2–3 times smaller in winter than in summer (mostly because of cloud screening, high SZAs and snow conditions). Thus, the monthly means calculated for winter months could be less representative of the actual NO_2 levels. In particular, the DOMINO NO_2 monthly means for November and January include only the last and first half of the month, respectively, because of the screening of the scenes with high SZA values (larger than 80°). In addition, for July and September, when relatively low monthly means are obtained from Pandora observations, the number of coincidences is about 3 times smaller than the other summer months, suggesting that these values are less statistically reliable. Pandora and surface concentration observations are sampled according to the SP overpasses.

Figure 6 shows the weekly cycle of the NO_2 total and tropospheric columns from OMI SP and DOMINO datasets. The weekly cycle from Pandora NO_2 total columns and surface concentrations from Helsinki-Kumpula air quality station are also included for comparison. The values are normalized with the weekly mean value in order to enhance the relative differences. The data correspond to the same overpasses presented in Fig. 5. All datasets show smaller values for the weekend compared to the other weekdays. This is expected because of the reduced emissions from car traffic and industrial activity during the weekend. NO_2 levels are usually slightly lower on Sunday than on Saturday. The amplitude of

the weekly cycle can be quantified as the percentage reduction between the weekend and weekdays. The NO_2 surface concentration is on average 40 % smaller at the weekend than on the weekdays. The amplitude of the weekly cycle become increasingly smaller for tropospheric and total columns (15–30 and 7–9 %, respectively, from OMI and 24 % for Pandora total columns). This dampening in the weekly cycle is expected because the surface concentrations are closer to the actual emission changes. The tropospheric column weekly cycle in Helsinki is similar but slightly smaller than the Europe average (amplitude about 40 %) as derived by Beirle et al. (2003). The weekly cycle values slightly increase when cloudy scenes are also taken into account, probably because of the larger number of winter observations included in the calculation.

4 Summary and conclusions

In this work, OMI NO_2 products have been compared against ground-based observations in Helsinki in order to evaluate their applicability for air quality monitoring at high latitudes. The main results of this comparison are summarized below.

- OMI SP NO_2 total columns agree on average within about ±5 % under clear-sky conditions with ground-based observations obtained from the Pandora spectrometer. The largest differences are observed for fall–winter days, which are characterized by cloudy conditions and large SZAs. OMI DOMINO NO_2 data show slightly smaller absolute values of NO_2 total column than SP, mainly because of different air mass factor values.

- The average difference values are the result of different factors that affect the comparison between OMI and ground-based total columns. The positive bias related to the overestimation of the slant columns and stratospheric vertical columns (as observed in the current OMI retrievals) is likely canceled by the underestimation expected from the dilution effect, caused by the relatively coarse OMI spatial resolution. The effect of different observing geometries on the surface reflectivity might further affect the comparison.

- OMI NO_2 total and tropospheric columns show a similar weekly cycle to the NO_2 surface concentrations in Helsinki, with smaller values at the weekend compared to the weekdays. Additionally, the weekly cycle observed from OMI total columns compares well with the one obtained from Pandora measurements.

- OMI tropospheric NO_2 seasonal cycle is similar to the one obtained from surface concentrations, while the total columns are strongly affected by the scarce number of data included in the monthly mean calculation. During fall–winter most of the data are screened as cloudy, and the resulting monthly means are typically characterized by large error bars.

- OMI cloud fraction values are used for selecting almost clear-sky scenes. OMI CFs below 0.5 give the same cloud-screening results as the ground-based cloud cover below 5/8 in more than 80 % of the cases.

In summary, despite relatively low NO_2 levels in Helsinki and frequent cloudy conditions (reducing the number of useful clear-sky observations), OMI NO_2 data have also been able to realistically represent air quality features at the surface at such high-latitude sites. The average differences are comparable to those obtained for midlatitude sites (see, e.g., Table 2 in Lamsal et al., 2014), with Pandora total columns usually higher than OMI retrievals. In the future, the next-generation OMI V3 retrievals (accounting for an improved spectral fitting procedure) will be more extensively evaluated against ground-based measurements.

The main limitations in using satellite data at high latitudes are related to the reduced light hours and large number of cloudy pixels during the fall–winter season. The weekly and seasonal cycles reported in this work are mostly obtained for spring or summertime conditions. A smaller pixel size would reduce the number of scenes screened as cloudy. A much smaller footprint will be achieved by the upcoming TROPOMI instrument (launch planned in October 2016), which will provide NO_2 observations with improved spatial resolution ($7 \times 7\,km^2$ at nadir) and signal-to-noise ratio. These features will be particularly important for monitoring the air quality of relatively small sources such as the city of Helsinki, and will increase the number of cloud-free pixels available for future analysis. Further studies will aim to validate TROPOMI observations when available using measurements from a new Pandora instrument recently installed at FMI. The effect of the snow/ice surface reflectivity information on the retrieval will also be analyzed.

5 Data availability

The OMI Standard Product NO_2 overpass file is publicly available from http://avdc.gsfc.nasa.gov/pub/data/satellite/Aura/OMI/V03/L2OVP/OMNO2/aura_omi_l2ovp_omno2_v03_helsinki.1.txt. The OMI DOMINO NO_2 overpass file is distributed by the TEMIS service at http://temis.nl/airpollution/no2col/data/omi/overpass/Helsinki_domino.dat. Surface concentration data have been downloaded from http://avaa.tdata.fi/web/smart/smear/download. Pandora NO_2 total columns are available upon request from the Finnish Meteorological Institute or from the first author.

The Supplement related to this article is available online at doi:10.5194/amt-9-5203-2016-supplement.

Acknowledgements. This work of Iolanda Ialongo was founded by the ILMA project (Applications of NO_2 satellite observations at high latitudes for monitoring air quality) within the ESA Living Planet Programme. Johanna Tamminen was partially funded by the Academy of Finland project INQUIRE. Folkert Boersma acknowledges support by the EU-FP7 grant QA4ECV (no. 607405). The authors acknowledge the NASA Earth Science Division and KNMI for funding the OMI NO_2 development and the archiving of standard and DOMINO products, respectively. The authors also thank the Atmospheric Sciences department of the University of Helsinki for providing surface concentration measurements through the SmartSMEAR download tool.

Edited by: B. N. Duncan
Reviewed by: two anonymous referees

References

Acarreta, J. R., de Haan, J. F., and Stammes, P.: Cloud pressure retrieval using the O2–O2 absorption band at 477 nm, J. Geophys. Res., 109, D05204, doi:10.1029/2003JD003915, 2004.

Adams, C., Normand, E. N., McLinden, C. A., Bourassa, A. E., Lloyd, N. D., Degenstein, D. A., Krotkov, N. A., Belmonte Rivas, M., Boersma, K. F., and Eskes, H.: Limb-nadir matching using non-coincident NO_2 observations: proof of concept and the OMI-minus-OSIRIS prototype product, Atmos. Meas. Tech., 9, 4103–4122, doi:10.5194/amt-9-4103-2016, 2016.

Beirle, S., Platt, U., Wenig, M., and Wagner, T.: Weekly cycle of NO_2 by GOME measurements: a signature of anthropogenic sources, Atmos. Chem. Phys., 3, 2225–2232, doi:10.5194/acp-3-2225-2003, 2003.

Beirle, S., Boersma, K. F., Platt, U., Lawrence, M. G., and Wagner, T.: Megacity emissions and lifetimes of nitrogen oxides probed from space, Science, 333, 1737–1739, doi:10.1126/science.1207824, 2011.

Belmonte Rivas, M., Veefkind, P., Boersma, F., Levelt, P., Eskes, H., and Gille, J.: Intercomparison of daytime stratospheric NO_2 satellite retrievals and model simulations, Atmos. Meas. Tech., 7, 2203–2225, doi:10.5194/amt-7-2203-2014, 2014.

Boersma, K. F., Jacob, D. J., Trainic, M., Rudich, Y., DeSmedt, I., Dirksen, R., and Eskes, H. J.: Validation of urban NO_2 concentrations and their diurnal and seasonal variations observed from the SCIAMACHY and OMI sensors using in situ surface measurements in Israeli cities, Atmos. Chem. Phys., 9, 3867–3879, doi:10.5194/acp-9-3867-2009, 2009.

Boersma, K. F., Eskes, H. J., Dirksen, R. J., van der A, R. J., Veefkind, J. P., Stammes, P., Huijnen, V., Kleipool, Q. L., Sneep, M., Claas, J., Leitão, J., Richter, A., Zhou, Y., and Brunner, D.: An improved tropospheric NO_2 column retrieval algorithm for the Ozone Monitoring Instrument, Atmos. Meas. Tech., 4, 1905–1928, doi:10.5194/amt-4-1905-2011, 2011.

Bucsela, E. J., Krotkov, N. A., Celarier, E. A., Lamsal, L. N., Swartz, W. H., Bhartia, P. K., Boersma, K. F., Veefkind, J. P., Gleason, J. F., and Pickering, K. E.: A new stratospheric and tropospheric NO_2 retrieval algorithm for nadir-viewing satellite instruments: applications to OMI, Atmos. Meas. Tech., 6, 2607–2626, doi:10.5194/amt-6-2607-2013, 2013.

Castellanos, P. and Boersma, K. F.: Reductions in nitrogen oxides over Europe driven by environmental policy and economic recession, Sci. Rep., 2, 265, doi:10.1038/srep00265, 2012.

Cede, A., Herman, J., Richter, A., Krotkov, N., and Burrows, J.: Measurements of nitrogen dioxide total column amounts at Goddard Space Flight Center using a Brewer spectrometer in direct sun mode, J. Geophys. Res., 111, D05304, doi:10.1029/2005JD006585, 2006.

de Foy, B., Lu, Z., Streets, D. G., Lamsal, L. K., and Duncan, B. N.: Estimates of power plant NO_x emissions and lifetimes from OMI NO_2 satellite retrievals, Atmos. Environ., 116, 1–11, doi:10.1016/j.atmosenv.2015.05.056, 2015.

de Ruyter de Wildt, M., Eskes, H., and Boersma, K. F.: The global economic cycle and satellite-derived NO_2 trends over shipping lanes, Geophys. Res. Lett., 39, L01802, doi:10.1029/2011GL049541, 2012.

Duncan, B. N., Yoshida, Y., de Foy, B., Lamsal, L. N., Streets, D. G., Lu, Z., Pickering, K. E., and Krotkov, N. A.: The observed response of Ozone Monitoring Instrument (OMI) NO_2 columns to NO_x emission controls on power plants in the United States: 2005–2011, Atmos. Environ., 81, 102–111, doi:10.1016/j.atmosenv.2013.08.068, 2013.

Ghude, S. D., Pfister, G. G., Jena, C., van der A, R. J., Emmons, L. K., and Kumar, R.: Satellite constraints of nitrogen oxide (NO_x) emissions from India based on OMI observations and WRF-Chem simulations, Geophys. Res. Lett., 40, 423–428, doi:10.1029/2012GL053926, 2013.

Herman, J., Cede, A., Spinei, E., Mount, G., Tzortziou, M., and Abuhassan, N.: NO_2 column amounts from ground-based Pandora and MFDOAS spectrometers using the direct-sun DOAS technique: Intercomparisons and application to OMI validation, J. Geophys. Res., 114, D13307, doi:10.1029/2009JD011848, 2009.

Hilboll, A., Richter, A., and Burrows, J. P.: Long-term changes of tropospheric NO_2 over megacities derived from multiple satellite instruments, Atmos. Chem. Phys., 13, 4145–4169, doi:10.5194/acp-13-4145-2013, 2013.

Ialongo, I., Hakkarainen, J., Hyttinen, N., Jalkanen, J.-P., Johansson, L., Boersma, K. F., Krotkov, N., and Tamminen, J.: Characterization of OMI tropospheric NO_2 over the Baltic Sea region, Atmos. Chem. Phys., 14, 7795–7805, doi:10.5194/acp-14-7795-2014, 2014.

Irie, H., Boersma, K. F., Kanaya, Y., Takashima, H., Pan, X., and Wang, Z. F.: Quantitative bias estimates for tropospheric NO_2 columns retrieved from SCIAMACHY, OMI, and GOME-2 using a common standard for East Asia, Atmos. Meas. Tech., 5, 2403–2411, doi:10.5194/amt-5-2403-2012, 2012.

Joiner, J. and Vasilkov, A. P.: First results from the OMI rotational raman scattering cloud pressure algorithm, IEEE T. Geosci. Remote, 44, 1272–1282, 2006.

Junninen, H., Lauri, A., Keronen, P., Aalto, P., Hiltunen, V., Hari, P., and Kulmala, M.: Smart-SMEAR: on-line data exploration and visualization tool for SMEAR stations, Boreal Environ. Res., 14, 447–457, 2009.

Kharol, S. K., Martin, R. V., Philip, S., Boys, B., Lamsal, L. N., Jerrett, M., Brauer, M., Crouse, D. L., McLinden, C., and Burnett, R. T.: Assessment of the magnitude and recent trends in satellite-derived ground-level nitrogen diox-

ide over North America, Atmos. Environ., 118, 236–245, doi:10.1016/j.atmosenv.2015.08.011, 2015.

Kleipool, Q. L., Dobber, M. R., de Haan, J. F., and Levelt, P. F.: Earth surface reflectance climatology from 3 years of OMI data, J. Geophys. Res., 113, D18308, doi:10.1029/2008JD010290, 2008.

Knepp, T., Pippin, M., Crawford, J., Chen, G., Szykman, J., Long, R., Cowen, L., Cede, A., Abuhassan, N., Herman, J., Delgado, R., Compton, J., Berkoff, T., Fishman, J., Martins, D., Stauffer, R., Thompson, A. M., Weinheimer, A., Knapp, D., Montzka, D., Lenschow, D., and Neil, D.: Estimating surface NO_2 and SO_2 mixing ratios from fast-response total column observations and potential application to geostationary missions, J. Atmos. Chem., 72, D15308, doi:10.1007/s10874-013-9257-6, 2013.

Krotkov, N. A., McLinden, C. A., Li, C., Lamsal, L. N., Celarier, E. A., Marchenko, S. V., Swartz, W. H., Bucsela, E. J., Joiner, J., Duncan, B. N., Boersma, K. F., Veefkind, J. P., Levelt, P. F., Fioletov, V. E., Dickerson, R. R., He, H., Lu, Z., and Streets, D. G.: Aura OMI observations of regional SO_2 and NO_2 pollution changes from 2005 to 2015, Atmos. Chem. Phys., 16, 4605–4629, doi:10.5194/acp-16-4605-2016, 2016.

Lamsal, L. N., Martin, R. V., Padmanabhan, A., van Donkelaar, A., Zhang, Q., Sioris, C. E., Chance, K., Kurosu, T. P., and Newchurch, M. J.: Application of satellite observations for timely updates to global anthropogenic NO_x emission inventories, Geophys. Res. Lett., 38, L05810, doi:10.1029/2010GL046476, 2011.

Lamsal, L. N., Martin, R. V., Parrish, D. D., and Krotkov, N. A.: Scaling relationship for NO_2 pollution and urban population size: a satellite perspective, Environ. Sci. Technol., 47, 7855–7861, doi:10.1021/es400744g, 2013.

Lamsal, L. N., Krotkov, N. A., Celarier, E. A., Swartz, W. H., Pickering, K. E., Bucsela, E. J., Gleason, J. F., Martin, R. V., Philip, S., Irie, H., Cede, A., Herman, J., Weinheimer, A., Szykman, J. J., and Knepp, T. N.: Evaluation of OMI operational standard NO_2 column retrievals using in situ and surface-based NO_2 observations, Atmos. Chem. Phys., 14, 11587–11609, doi:10.5194/acp-14-11587-2014, 2014.

Levelt, P. F., van den Oord, G. H. J., Dobber, M. R., Malkki, A., Visser, H., de Vries, J., Stammes, P., Lundell, J. O. V., and Saari, H.: The Ozone Monitoring Instrument, IEEE T. Geosci. Remote, 44, 1093–1101, doi:10.1109/TGRS.2006.872333, 2006.

Lin, J.-T., Martin, R. V., Boersma, K. F., Sneep, M., Stammes, P., Spurr, R., Wang, P., Van Roozendael, M., Clémer, K., and Irie, H.: Retrieving tropospheric nitrogen dioxide from the Ozone Monitoring Instrument: effects of aerosols, surface reflectance anisotropy, and vertical profile of nitrogen dioxide, Atmos. Chem. Phys., 14, 1441–1461, doi:10.5194/acp-14-1441-2014, 2014.

Liu, F., Beirle, S., Zhang, Q., Dörner, S., He, K., and Wagner, T.: NO_x lifetimes and emissions of cities and power plants in polluted background estimated by satellite observations, Atmos. Chem. Phys., 16, 5283–5298, doi:10.5194/acp-16-5283-2016, 2016.

Lu, Z., Streets, D. G., de Foy, B., Lamsal, L. N., Duncan, B. N., and Xing, J.: Emissions of nitrogen oxides from US urban areas: estimation from Ozone Monitoring Instrument retrievals for 2005–2014, Atmos. Chem. Phys., 15, 10367–10383, doi:10.5194/acp-15-10367-2015, 2015.

Marchenko, S., Krotkov, N. A., Lamsal, L. N., Celarier, E. A., Swartz, W. H., and Bucsela, E. J.: Revising the slant column density retrieval of nitrogen dioxide observed by the Ozone Monitoring Instrument, J. Geophys. Res.-Atmos., 120, 1–23, doi:10.1002/2014JD022913, 2015.

McLinden, C. A., Fioletov, V., Boersma, K. F., Krotkov, N., Sioris, C. E., Veefkind, J. P., and Yang, K.: Air quality over the Canadian oil sands: A first assessment using satellite observations, Geophys. Res. Lett., 39, L04804, doi:10.1029/2011GL050273, 2012.

McLinden, C. A., Fioletov, V., Boersma, K. F., Kharol, S. K., Krotkov, N., Lamsal, L., Makar, P. A., Martin, R. V., Veefkind, J. P., and Yang, K.: Improved satellite retrievals of NO_2 and SO_2 over the Canadian oil sands and comparisons with surface measurements, Atmos. Chem. Phys., 14, 3637–3656, doi:10.5194/acp-14-3637-2014, 2014.

McLinden, C. A., Fioletov, V., Shephard, M. W., Krotkov, N., Li, C., Martin, R. V., Moran, M. D., and Joiner, J.: Space-based detection of missing sulfur dioxide sources of global air pollution, Nat. Geosci., 9, 496–500, doi:10.1038/ngeo2724, 2016.

Stammes, P., Sneep, M., de Haan, J. F., Veefkind, J. P., Wang, P., and Levelt, P. F.: Effective cloud fractions from the Ozone Monitoring Instrument: Theoretical framework and validation, J. Geophys. Res., 113, D16S38, doi:10.1029/2007JD008820, 2008.

Streets, D. G., Canty, T., Carmichael, G. R., de Foy, B., Dickerson, R. R., Duncan, B. N., Edwards, D. P., Haynes, J. A., Henze, D. K., Houyoux, M. R., Jacob, D. J., Krotkov, N. A., Lamsal, L. N., Liu, Y., Lu, Z., Martin, R. V., Pfister, G. G., Pinder, R. W., Salawitch, R. J., and Wecht, K. J.: Emissions estimation from satellite retrievals: a review of current capability, Atmos. Environ., 77, 1011–1042, doi:10.1016/j.atmosenv.2013.05.051, 2013.

Tzortziou M., Herman, J. R., Loughner, C. P., Cede, A., Abuhassan, N., and Naik, S.: Spatial and temporal variability of ozone and nitrogen dioxide over a major urban estuarine ecosystem, J. Atmos. Chem., Special Issue PINESAP, DISCOVER-AQ, doi:10.1007/s10874-013-9255-8, 2013.

Vandaele, A. C., Hermans, C., Simon, P. C., Carleer, M., Colin, R., Fally, S., Mérienne, M. F., Jenouvrier, A., and Coquart, B.: Measurements of the NO_2 absorption cross-section from 42000 cm^{-1} to 10000 cm^{-1} (238–1000 nm) at 220 K and 294 K, J. Quant. Spectrosc. Ra., 59, 171–184, 1988.

van Geffen, J. H. G. M., Boersma, K. F., Van Roozendael, M., Hendrick, F., Mahieu, E., De Smedt, I., Sneep, M., and Veefkind, J. P.: Improved spectral fitting of nitrogen dioxide from OMI in the 405–465 nm window, Atmos. Meas. Tech., 8, 1685–1699, doi:10.5194/amt-8-1685-2015, 2015.

Vasilkov, A., Qin, W., Krotkov, N., Lamsal, L., Spurr, R., Haffner, D., Joiner, J., Yang, E.-S., and Marchenko, S.: Accounting for the effects of surface BRDF on satellite cloud and trace-gas retrievals: A new approach based on geometry-dependent Lambertian-equivalent reflectivity applied to OMI algorithms, Atmos. Meas. Tech. Discuss., doi:10.5194/amt-2016-133, in review, 2016.

Vinken, G. C. M., Boersma, K. F., van Donkelaar, A., and Zhang, L.: Constraints on ship NO_x emissions in Europe using GEOS-Chem and OMI satellite NO_2 observations, Atmos. Chem. Phys., 14, 1353–1369, doi:10.5194/acp-14-1353-2014, 2014.